

# Influence of the surface adsorption–desorption processes on the ignition curves of volatile organic compounds (VOCs) complete oxidation over supported catalysts

M. Paulis<sup>a</sup>, L.M. Gandía<sup>b</sup>, A. Gil<sup>b</sup>, J. Sambeth<sup>c</sup>, J.A. Odriozola<sup>c</sup>, M. Montes<sup>a,\*</sup>

<sup>a</sup> *Grupo de Ingeniería Química, Fac. de C. Químicas, UPV-EHU, Apdo 1072, E-20080 San Sebastián, Spain*

<sup>b</sup> *Departamento de Química Aplicada, Universidad Pública de Navarra, Campus de Arrosadía s/n, E-31006 Pamplona, Spain*

<sup>c</sup> *Departamento de Q. Inorgánica e Instituto de C. de Materiales, Universidad de Sevilla, Av. A. Vespucio s/n, E-41092 Sevilla, Spain*

Received 30 April 1999; received in revised form 28 November 1999; accepted 18 December 1999

## Abstract

The simplicity to obtain ignition curves has resulted in their extended use for the measurement of the catalysts activity in the complete oxidation of VOCs. However, we have found that this method gives incorrect results for some systems, such as conversions greater than 100% or disagreements between the conversion values calculated through the concentration change of the reactants and the products, which can lead to misunderstandings. Toluene oxidation over reduced Pd/Al<sub>2</sub>O<sub>3</sub> and acetone oxidation over supported Mn<sub>2</sub>O<sub>3</sub> have presented those features. The study of these systems has been carried out performing DRIFTS spectra under reaction conditions and TPD experiments. The effect of the start-up procedure of the complete oxidation reactions has been considered as well. After discarding the formation of partial oxidation products and the hydrogen retention on Pd as possible causes, the adsorption–desorption processes of VOCs, surface intermediates and CO<sub>2</sub> were considered. It can be concluded that when the activity of the active phase supported on the Al<sub>2</sub>O<sub>3</sub> is high enough to allow the coupling at relatively low temperature of combustion with the adsorption and desorption processes of toluene or acetone and CO<sub>2</sub>, a sort of chain reaction occurs leading to CO<sub>2</sub> peaks. ©2000 Elsevier Science B.V. All rights reserved.

*Keywords:* Acetone and toluene complete oxidation; Adsorption–desorption processes; Light-off curves; Supported Pd and Mn<sub>2</sub>O<sub>3</sub> catalysts; Volatile organic compounds

## 1. Introduction

The catalytic combustion of volatile organic compounds (VOCs) is becoming of increasing importance in pollution emission control. Both supported noble metals and transition metal oxides have been used as catalysts for these reactions [1]. Supported noble

metals are usually more active for VOCs complete oxidation, however, transition metal oxides are cheaper and can achieve higher thermal stability and greater resistance to poisoning [2]. Among the noble metals, supported Pt and Pd are the most widely used catalysts for VOCs combustion, due to their high intrinsic activity [3,4]. In the case of the transition metal oxides, those of Mn and Co are well known as the most active among the single oxides for complete oxidation [5,6]. In spite of the lower activity of these materials compared with that of the noble metals, their relatively low

\* Corresponding author. Tel.: +34-943-018183; fax: +34-943-212236.

E-mail address: qppmoram@sc.ehu.es (M. Montes).

cost has spurred considerable effort in search of suitable combustion catalysts based on transition metal oxides, such as some perovskites and other mixed oxides [7–9].

Ignition or light-off curves are the most wide-spread way of catalytic activity evaluation in VOCs complete oxidation studies. These curves simply depict the VOC conversion versus reaction temperature. The conversion can be calculated by measuring the extent of VOC removal, or alternatively, by the increase of total oxidation products ( $\text{CO}_2$  and  $\text{H}_2\text{O}$ ) concentration that take place in the gaseous stream as reaction temperature increases. A good agreement between the two procedures can be expected when complete oxidation is the only reaction pathway; that is, without partial oxidation products formation and in absence of phenomena related with reactant and products adsorption or retention. Few examples exist in the literature reporting open mass balances during the catalytic combustion of VOCs other than those due to the presence of partial oxidation activity. Heyes et al. [10] when studying butanal combustion over  $\text{Co}_3\text{O}_4$ ,  $\text{MnO}_2$ ,  $\text{CuO}$  and Pt-honeycomb catalysts measured noticeably higher conversions by means of the butanal removal than by  $\text{CO}_2$  appearance. This was only in part due to  $\text{CO}$  formation. Imamura et al. [11] reported toluene conversions to  $\text{CO}_2$  over Sm containing  $\text{Co}_3\text{O}_4$  that exceeded 100% in some cases as a result of the combustion of carbonaceous deposit on the surface of the catalyst. Papaefthimiou et al. [4] and Lahousse et al. [12] studied the combustion of benzene, butanol, *n*-hexane and ethyl acetate over supported group VIII metal catalysts. These authors found that  $\text{CO}_2$  and  $\text{H}_2\text{O}$  were the only reaction products and that the result of the carbon balance strongly depended on the VOC molecule, the reaction temperature and some catalyst properties. Thus, when the support consisted in low-surface-area  $\alpha\text{-Al}_2\text{O}_3$  the carbon balance was always well satisfied. On the contrary, in the case of catalysts supported on high-surface-area carriers and especially at low combustion temperatures significantly higher butanol and ethyl acetate conversions were measured by means of the VOC removal than by  $\text{CO}_2$  appearance. It was found that these results were due to VOCs and heavy by-products adsorption and accumulation on the support.

The main goal in this work is to study some anomalous behaviours in complete oxidation ignition curves

of acetone over alumina- and silica-supported  $\text{Mn}_2\text{O}_3$  and toluene over reduced  $\text{Pd}/\text{Al}_2\text{O}_3$ , such as disagreements between the conversion calculated through the concentration changes of the reactants and the products, or conversions exceeding 100%. The materials are typical VOCs combustion catalysts and the molecules have been selected as representative of the aromatic and carbonyl compounds, respectively.

## 2. Experimental

The  $\text{Pd}/\text{Al}_2\text{O}_3$  catalyst was prepared by the incipient wetness impregnation of  $\gamma\text{-Al}_2\text{O}_3$  (Spheralite 505, Procatalyse; 100–200  $\mu\text{m}$  particle size fraction) with an aqueous solution of  $\text{Pd}(\text{NO}_3)_2$  (Johnson Matthey, Alfa). The Pd loading was 1% by weight. The catalyst was dried at 393 K for 16 h and calcined at 773 K for 2 h in air. The  $\text{Mn}_2\text{O}_3/\text{SiO}_2$  and  $\text{Mn}_2\text{O}_3/\text{Al}_2\text{O}_3$  catalysts were prepared by dry impregnation of the 200–300  $\mu\text{m}$  particle size fraction of the supports ( $\text{SiO}_2$  AF125, Kali Chemie ( $304 \text{ m}^2 \text{ g}^{-1}$ ), and  $\gamma\text{-Al}_2\text{O}_3$  Spheralite 505, Procatalyse ( $185 \text{ m}^2 \text{ g}^{-1}$ )). However, in this case two different aqueous impregnation solutions were used. The first one contained manganese nitrate ( $\text{Mn}(\text{NO}_3)_2 \cdot 4\text{H}_2\text{O}$  Merck, PA) only (named (N)) and the second one contained citric acid (Panreac, PA) in addition to the manganese salt (named (C)). The same amount of citric acid and manganese (II) nitrate equivalents were mixed and brought to the boiling point for 30 min. After the impregnation, the solids were dried under vacuum (0.05 bar) at 343 K for 8 h and calcined at 823 K for 4 h in a muffle. Manganese contents were determined by atomic absorption spectroscopy using a Perkin–Elmer 2100 spectrophotometer. The resulting values were in the 5.7 to 6.5 Mn wt.% range.

The BET specific surface areas were measured by nitrogen adsorption at 77 K using an automatic volumetric apparatus (Micromeritics ASAP 2000). Samples were previously degassed for 8 h at 473 K and  $10^{-3}$  Torr. The Pd dispersion was measured by  $\text{H}_2$  chemisorption at 353 K (Micromeritics Pulse Chemisorb 2700). The PdO and  $\text{Mn}_2\text{O}_3$  mean crystallite diameters were estimated from application of the Scherrer equation to the X-ray Diffraction (XRD) patterns (Philips APD 1710 and Siemens D-500 powder diffractometers using  $\text{Cu K}_\alpha$  filtered radiation).

The width of the PdO (101) and Mn<sub>2</sub>O<sub>3</sub> (222) peaks at half-maximum was corrected for K<sub>α</sub> doublet and instrumental broadening.

Toluene and acetone complete oxidation reactions were carried out in a tubular fixed-bed reactor at atmospheric pressure. Mass flow controllers (Brooks 5850TR, Bronkhorst High-Tec) were used to prepare the feed mixture. Ar (SEO 99.999%) or air (SEO 99.999%) was bubbled through two thermostated and pressurised saturators containing either toluene (Fluka, puriss. p.a.) or acetone (Panreac, PA). This stream was further mixed with air in order to set the feed stream composition at 225 ppmv (toluene) or 600 ppmv (acetone) and passed through the catalyst placed on the top of a carborundum bed. This configuration was designed to pre-mix and pre-heat the stream entering the reactor, and thus obtaining a homogeneous temperature, measured by a thermocouple placed just in the beginning of the catalytic bed. The reactor was surrounded by an electrical furnace equipped with a temperature programmer. Toluene oxidation over Pd/Al<sub>2</sub>O<sub>3</sub> was carried out at a W/Q<sub>A0</sub> ratio of 1.7 (g<sub>catalyst</sub> min cm<sup>-3</sup><sub>toluene NPT</sub>), with 200 mg of catalyst and a total gas flow rate of 510 cm<sup>3</sup> min<sup>-1</sup>. Acetone oxidation reactions over supported Mn<sub>2</sub>O<sub>3</sub> catalysts were performed at an identical W/Q<sub>A0</sub> of 0.08 (g<sub>Mn</sub> min cm<sup>-3</sup><sub>acetone NPT</sub>) referred to the amount of Mn loaded into the reactor, with a catalyst weight varying between 220 and 250 mg depending on the Mn content of the catalyst, and a total gas flow rate of 280 cm<sup>3</sup> min<sup>-1</sup>. The ignition curves were constructed following both the VOC disappearance and the CO<sub>2</sub> appearance at a controlled heating rate of 2.5 K min<sup>-1</sup>. Analyses were done by on-line gas chromatography (GC, Hewlett Packard 6890). In the case of toluene complete oxidation reactions, a thermal conductivity detector (TCD) was used for toluene and H<sub>2</sub>O (TR-WAX 30 m column) quantification. The CO<sub>2</sub> concentration was continuously monitored by means of an IR analyser (Digital Control Systems Model 300). Similarly, in the case of the acetone complete oxidation reactions, a flame ionisation detector (FID) was used for acetone (HP column 19091N-113, HP-INNOWax 30 m×0.32 mm ID) analyses and a TCD was used for CO<sub>2</sub> (HP column 19001A-Q01-6000, 6 ft HayeSep Q) quantification. The sensitivity of the GC-FID was better than 5 ppmv of acetone.

The catalysts were treated under 100 cm<sup>3</sup><sub>air</sub> min<sup>-1</sup> at 573 K for 1 h before reaction, and then cooled down in air to the starting reaction temperature. In the case of Pd/Al<sub>2</sub>O<sub>3</sub>, H<sub>2</sub> and Ar pretreatments at 573 K were carried as well. Acetone oxidation reactions over supported Mn<sub>2</sub>O<sub>3</sub> were started up according to two distinct procedures that will be named ‘unstable’ (u) and ‘stable’ (s), respectively, with respect to acetone adsorption on the catalyst surface as explained later on. In the first case (u), once the air treatment has finished, the catalytic bed is allowed to steadily reach the starting reaction temperature (413 K) under 100 cm<sup>3</sup><sub>air</sub> min<sup>-1</sup>. Then, the acetone-air mixture is fed into the reactor using a 6-way valve at the same time as the temperature ramp is switched on. In the second one (s), however, the catalytic bed is stabilised for 3 h at 413 K under the feed stream before the temperature starts to increase. All the toluene oxidation reactions began at 373 K according to a procedure similar to that so-called (s), after the toluene GC signal became constant.

The toluene and CO<sub>2</sub> TPD experiments were carried under the same conditions used to obtain the ignition curves, analysing the products by on-line mass spectrometry (Omnistar, Balzers). The sensitivity of the mass spectrometer was better than 5 ppmv of toluene.

DRIFTS spectra under reaction conditions were obtained by using a controlled-temperature and environment diffuse reflectance DRIFTS chamber (SPECTRA TECH 0030-102) with ZnSe windows in a Nicolet 510P infrared spectrometer with KBr optics and DTGS detector [13]. The Pd/Al<sub>2</sub>O<sub>3</sub> catalysts were subjected to an air or H<sub>2</sub> (65 cm<sup>3</sup> min<sup>-1</sup>) pretreatment at 573 K during 30 min. Then the temperature was cooled down to room temperature and a mixture of 225 ppm of toluene in air (2.5 cm<sup>3</sup> min<sup>-1</sup>) was introduced. The reaction process was analysed in the temperature range from 298 to 673 K.

### 3. Results and discussion

The results of the physicochemical characterisation of the catalysts are given in Table 1. The XRD patterns of the supported Mn catalysts calcined at 823 K showed the presence of a well-crystallised Mn<sub>2</sub>O<sub>3</sub> phase. The use of an impregnation solution containing citric acid favoured a higher dispersion of Mn<sub>2</sub>O<sub>3</sub> over

Table 1  
Specific surface areas  $S_{\text{BET}}$  ( $\text{m}^2/\text{g}$ ), metallic contents and mean crystallite sizes of the prepared supported catalysts

Catalyst	$S_{\text{BET}}$ ( $\text{m}^2/\text{g}$ )	Pd or Mn (%)	$d_{\text{XRD}}$ (nm)
Pd/Al <sub>2</sub> O <sub>3</sub>	202	1.0	4.2
Mn <sub>2</sub> O <sub>3</sub> /Al <sub>2</sub> O <sub>3</sub> (N)	86	6.11	22.7
Mn <sub>2</sub> O <sub>3</sub> /Al <sub>2</sub> O <sub>3</sub> (C)	88	5.69	14.8
Mn <sub>2</sub> O <sub>3</sub> /SiO <sub>2</sub> (N)	274	6.11	17.8
Mn <sub>2</sub> O <sub>3</sub> /SiO <sub>2</sub> (C)	269	6.50	12.4

both supports, as deduced from the smaller mean crystallite diameters measured by XRD line broadening. In the case of Pd/Al<sub>2</sub>O<sub>3</sub> the dispersion was 32% by H<sub>2</sub> chemisorption corresponding to a particle diameter of 3.5 nm, and the XRD pattern of the calcined sample showed that PdO was the predominant Pd phase having a mean crystallite diameter of 4.2 nm.

The ignition curves for toluene complete oxidation over Pd/Al<sub>2</sub>O<sub>3</sub> pretreated in air or in H<sub>2</sub> are shown in Fig. 1. The H<sub>2</sub> reduction gives rise to a much more active catalyst with a  $T_{50}$ , temperature at which conversion reaches 50%, more than 100 K lower than that of the catalyst pretreated in air. It is remarkable that the conversion calculated from the CO<sub>2</sub> signal for the reduced Pd/Al<sub>2</sub>O<sub>3</sub> sample reaches approximately 200% (CO<sub>2</sub> peak) at 450 K. Furthermore, an important disagreement with respect to the conversion measured by toluene disappearance is apparent in this case, which

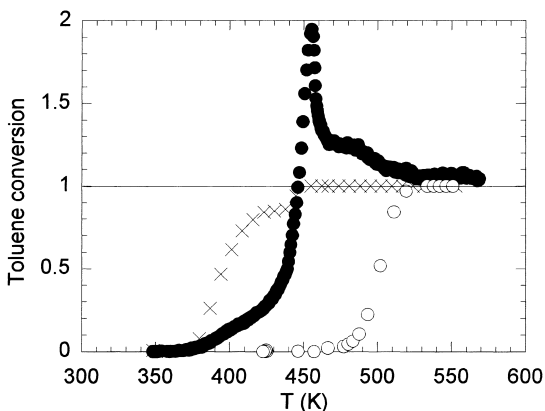


Fig. 1. Ignition curves for toluene complete oxidation over Pd/Al<sub>2</sub>O<sub>3</sub> pretreated in air (○) and in H<sub>2</sub> (×, ●) at 573 K. Toluene fractional conversions were calculated through toluene disappearance (○ and ×) and CO<sub>2</sub> appearance (●).

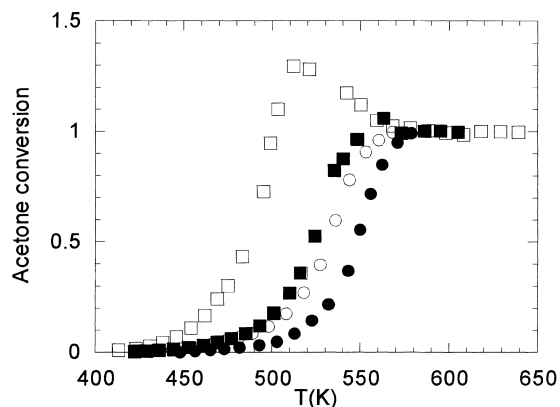


Fig. 2. Ignition curves for acetone complete oxidation over supported Mn<sub>2</sub>O<sub>3</sub> catalysts according to the start-up procedure (s). Acetone fractional conversions were calculated through CO<sub>2</sub> appearance. (●) Mn<sub>2</sub>O<sub>3</sub>/SiO<sub>2</sub> (N), (■) Mn<sub>2</sub>O<sub>3</sub>/SiO<sub>2</sub> (C), (○) Mn<sub>2</sub>O<sub>3</sub>/Al<sub>2</sub>O<sub>3</sub> (N), (□) Mn<sub>2</sub>O<sub>3</sub>/Al<sub>2</sub>O<sub>3</sub> (C).

results in significantly higher toluene conversions with this last calculus method below 450 K.

The ignition curves for acetone complete oxidation over supported Mn<sub>2</sub>O<sub>3</sub> catalysts using the CO<sub>2</sub> signal according to the start-up procedure (s) are given in Fig. 2. As it can be seen for both alumina and silica supports, the catalysts prepared from the manganese citrate precursor are more active than those prepared from manganese nitrate. This result is well accounted for by the fact that better dispersed Mn<sub>2</sub>O<sub>3</sub> catalysts result from impregnating both alumina and silica with citric acid-containing solutions, as it can be inferred from the mean Mn<sub>2</sub>O<sub>3</sub> crystallite sizes included in Table 1. In spite of their slightly higher Mn<sub>2</sub>O<sub>3</sub> crystallite size, the alumina-supported Mn<sub>2</sub>O<sub>3</sub> catalysts are more active than their silica-supported counterparts, which suggests that dispersion is not the only factor controlling catalytic activity. The use of the citrate precursor gives a decrease of the  $T_{50}$  value by approximately 25 K for Mn<sub>2</sub>O<sub>3</sub>/SiO<sub>2</sub> and up to 50 K for Mn<sub>2</sub>O<sub>3</sub>/Al<sub>2</sub>O<sub>3</sub> with respect to the catalysts prepared from manganese nitrate. As a result, Mn<sub>2</sub>O<sub>3</sub>/Al<sub>2</sub>O<sub>3</sub> (C) becomes the most active supported Mn<sub>2</sub>O<sub>3</sub> catalyst prepared, with a relatively low  $T_{50}$  of 485 K. CO<sub>2</sub> peaks were also observed during acetone oxidation with the most active Mn catalysts; those prepared from manganese citrate precursor. In this way, the conversion reaches about 130% at 510 K over Mn<sub>2</sub>O<sub>3</sub>/Al<sub>2</sub>O<sub>3</sub> (C) and around 110% at 560 K over Mn<sub>2</sub>O<sub>3</sub>/SiO<sub>2</sub> (C).

After the presentation of the complete oxidation ignition curves of acetone over alumina- and silica-supported  $\text{Mn}_2\text{O}_3$  and toluene over reduced  $\text{Pd}/\text{Al}_2\text{O}_3$ , some possible explanations for the  $\text{CO}_2$  peaks and disagreements between the conversion values could be proposed:

### 3.1. Partial oxidation

Obviously toluene partial oxidation could account for the higher conversions measured for reduced  $\text{Pd}/\text{Al}_2\text{O}_3$  following the toluene removal from the products stream. Alternatively, a mass spectrometer was used to follow the reaction products instead of the GC with the TCD detector. This analytical technique presents several advantages over others, even if the sensitivity is not so high: quick responses for temperature programmed techniques and no need of previous knowledge of the products. There have not been detected any reaction products other than  $\text{CO}_2$  and  $\text{H}_2\text{O}$  by on-line mass spectrometry. This technique allows us to detect selectivities as low as 2%, therefore, conversion disagreements of 60% as the ones seen in Fig. 1 cannot be explained by the formation of partial oxidation products.

### 3.2. $\text{H}_2$ retention

Palladium is known to retain considerable amounts of  $\text{H}_2$  after reduction, and the presence of that  $\text{H}_2$  during the oxidation reaction could lead to modifications of the catalytic behaviour of  $\text{Pd}/\text{Al}_2\text{O}_3$ , due to temperature run-ups produced by the release of  $\text{H}_2$  in the oxidative atmosphere. Nevertheless, no  $\text{H}_2$  desorption has been found in TPD experiments carried out at the same conditions of the reactions, i.e. purging the sample in an inert stream at a temperature 10 K above that of the reduction and cooling the sample in the inert stream. Furthermore the pretreatment in Ar of  $\text{Pd}/\text{Al}_2\text{O}_3$ , which produces an active Pd phase as well [14], resulted in the same ignition curve features as the reduced  $\text{Pd}/\text{Al}_2\text{O}_3$ .

### 3.3. Adsorption–desorption processes

A third hypothesis related to the desorption of reactants or products retained by the catalyst can be

proposed. Several experiments were designed and performed in order to check this hypothesis.

#### 3.3.1. DRIFTS data

DRIFTS spectra of the adsorbed species during the oxidation of toluene over reduced  $\text{Pd}/\text{Al}_2\text{O}_3$  were obtained at the same experimental conditions used in the catalytic tests. The infrared spectra of the adsorbed species on reduced  $\text{Pd}/\text{Al}_2\text{O}_3$  at increasing temperatures are given in Fig. 3. Bands associated with the adsorption of toluene ( $1604$  and  $1498\text{ cm}^{-1}$ ) are observed up to 423 K. The temperature ramp brings about new species on the surface, probably due to intermediates of the oxidation reaction such as carboxylates ( $1560$ ,  $1427$  and  $1380\text{ cm}^{-1}$ ), from temperatures as low as 373 K [15–17]. Busca et al. [18,19] had already detected the presence of adsorbed carboxylate species during the complete oxidation of propane and butane. In the case of toluene complete oxidation, the carboxylate species could easily be benzoates at the early stages of the reaction, as one of the steps in the complete oxidation mechanism proposed by Lars and Andersson [20]. These carboxylate species remain at high temperature, indicating that they have become spec-

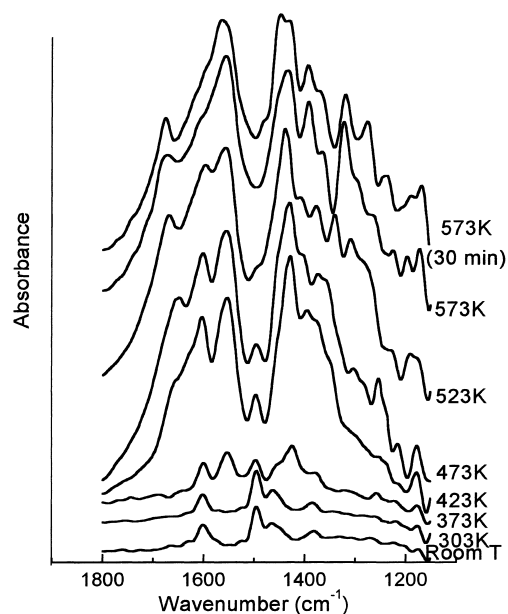


Fig. 3. DRIFTS spectra of toluene complete oxidation over reduced  $\text{Pd}/\text{Al}_2\text{O}_3$  at increasing temperatures.

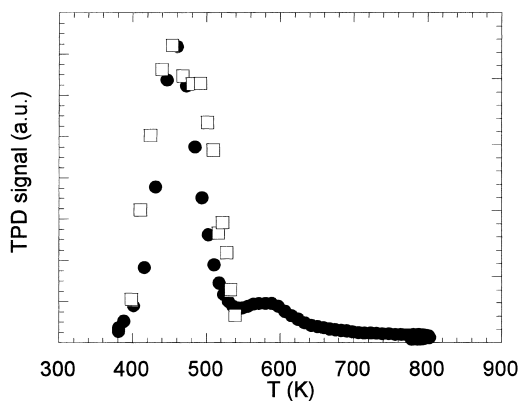


Fig. 4. Temperature programmed desorption curves of  $m/z=91$ ; toluene ( $\square$ ) and  $m/z=44$ ;  $\text{CO}_2$  ( $\bullet$ ) over  $\text{Al}_2\text{O}_3$ .

tators of the reaction at some stage. However, what seems to be clear is that at temperatures as low as 373 K, the formation of carboxylates and subsequently the start of the oxidation activity of reduced  $\text{Pd}/\text{Al}_2\text{O}_3$  overlaps with the desorption of toluene.

### 3.3.2. $\text{CO}_2$ and toluene TPD

Moreover, toluene and  $\text{CO}_2$  TPD experiments were carried out over the  $\text{Al}_2\text{O}_3$  support and evaluated by mass spectrometry as shown in Fig. 4.  $\text{CO}_2$  ( $m/z=44$ ) was adsorbed on  $\text{Al}_2\text{O}_3$  at 373 K (the starting temperature of the ignition curves), desorbing in two peaks, the big one at 460 K and a small one at 580 K. Toluene ( $m/z=91$ ) was also adsorbed on  $\text{Al}_2\text{O}_3$  at 373 K and desorbed around 450 K. So if the oxidation of toluene on reduced  $\text{Pd}/\text{Al}_2\text{O}_3$  takes place at temperatures below 520 K, the reaction itself will be coupled with the adsorption–desorption of toluene and  $\text{CO}_2$  on the support. Similar TPD experiments carried out on reduced  $\text{Pd}/\text{Al}_2\text{O}_3$  brought about the formation of several products (benzene and  $\text{CH}_4$ ) not found in the oxidising environment of the reaction.

### 3.3.3. Start-up procedure

In the case of the acetone oxidation over supported Mn catalysts, the adsorption–desorption processes of the reactant and the products could also play an important role. In this context it is interesting to analyse the results obtained as a function of the start-up procedure followed. The ignition curves for acetone complete oxidation with the  $\text{Mn}_2\text{O}_3/\text{SiO}_2$  (N) and

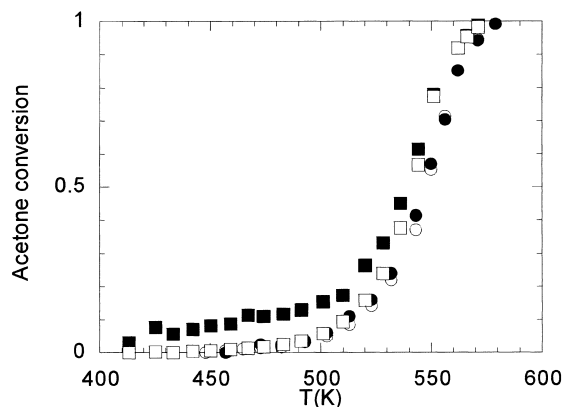


Fig. 5. Ignition curves for acetone complete oxidation over  $\text{Mn}_2\text{O}_3/\text{SiO}_2$  (N) according to the start-up procedures (s) (circles) and (u) (squares). Acetone fractional conversions were calculated through acetone disappearance (filled symbols) and  $\text{CO}_2$  appearance (open symbols).

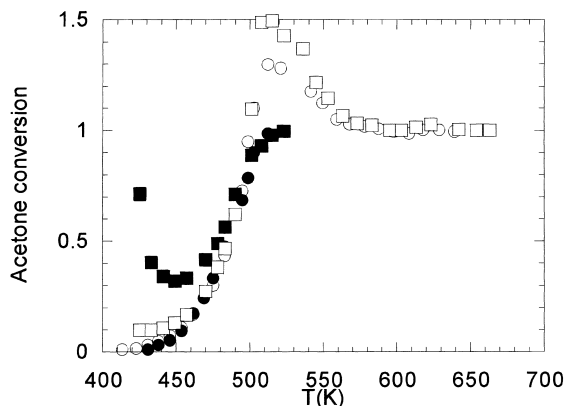


Fig. 6. Ignition curves for acetone complete oxidation over  $\text{Mn}_2\text{O}_3/\text{Al}_2\text{O}_3$  (C) according to the start-up procedures (s) (circles) and (u) (squares). Acetone fractional conversions were calculated through acetone disappearance (filled symbols) and  $\text{CO}_2$  appearance (open symbols).

$\text{Mn}_2\text{O}_3/\text{Al}_2\text{O}_3$  (C) catalysts have been included in Figs. 5 and 6, respectively; these are the solids that showed the lowest and highest activities among the supported Mn catalysts prepared. As it can be seen in Fig. 5, an excellent agreement exists between the acetone conversions calculated through both acetone removal and  $\text{CO}_2$  appearance over  $\text{Mn}_2\text{O}_3/\text{SiO}_2$  (N) when the reaction starts according to the (s) procedure. It should be noted that in this case the

acetone-air mixture was previously in contact with the catalyst for 3 h at 413 K. However, if the (u) procedure is used to start the reaction, then discrepancies between some conversion results arise. Now, whereas the conversion calculated by means of the CO<sub>2</sub> appearance is close to that obtained before with the (s) procedure, the values calculated through the acetone disappearance exceed moderately the previous ones along the low-temperature range of the ignition curve. The low activity of this catalyst with a  $T_{50}$  value of approximately 550 K is accompanied by the absence of CO<sub>2</sub> peaks during acetone combustion. The Mn<sub>2</sub>O<sub>3</sub>/Al<sub>2</sub>O<sub>3</sub> (C) catalyst, on the other hand, is considerably more active (see Fig. 2,  $T_{50}$ =485 K) and the corresponding ignition curves have a striking behaviour, as shown in Fig. 6. In this case, the start-up procedure (s) results in coincident conversions until the ignition point is attained. Then, acetone conversions calculated from CO<sub>2</sub> appearance clearly surpass those obtained through the VOC removal, giving rise to a CO<sub>2</sub> peak of 130% conversion at 510 K. However, if reaction begins without previously contacting the acetone-air mixture with the catalyst surface ((u) procedure) serious discrepancies arise immediately. Conversions of 10% (from CO<sub>2</sub>) and even as high as 70% (from acetone) are measured at very low reaction temperatures. A marked CO<sub>2</sub> peak of 150% conversion is also observed at 510 K. Taking into account the differences between the two start-up procedures used, the results strongly suggest that a considerable amount of acetone can be retained by the catalyst without being oxidised at reaction temperatures below the ignition point. This could explain the discrepancies observed at high conversions when calculated from acetone disappearance after a start-up according to the (u) procedure. On the other hand, during the start-up named (s) acetone adsorption presumably takes place during the 3 h period before the temperature ramp starts which results in good agreement between conversion values afterwards. Adsorption of VOCs and heavy by-products on supported catalysts has been found by Papaefthimiou et al. [4] and Lahousse et al. [12] for systems also showing discrepancies between the conversion results. According to the authors, these phenomena are reflected in transient periods as high as 16 h due to the typical very low concentration of the VOC molecule in the feed. Several routes leading to acetone retention could be

proposed. Finocchio et al. [21] had shown that molecularly adsorbed acetone starts to be oxidised on the surface of some transition metal oxides above 373 K, giving rise mainly to adsorbed acetate species in the 373–473 K range. It should be noticed that these temperatures are just below the  $T_{50}$  value of 485 K of the very active Mn<sub>2</sub>O<sub>3</sub>/Al<sub>2</sub>O<sub>3</sub> (C) catalyst. In addition, as pointed out by Busca et al. [19] carbonyl compounds such as acetone that carry hydrogen atoms at the  $\alpha$  position can undergo base- or acid-catalysed enolization at the surface of the metal oxides yielding strongly bound enolate anions. Obviously, this makes a way to the formation of aldol condensation products of acetone that can remain adsorbed on the catalyst surface also, as it is the case with Al<sub>2</sub>O<sub>3</sub> at the noticeable low temperature of 373 K [22]. Due to the nature of the VOC molecule an important effect of the acid-base properties of the catalyst on the amount of acetone retained is expected. This is probably related with the higher acetone retention observed over Mn<sub>2</sub>O<sub>3</sub> supported on Al<sub>2</sub>O<sub>3</sub> than SiO<sub>2</sub>, and also when the impregnation solution contained citric acid than the manganese nitrate precursor only. In this case, an indirect measure of the retained acetone is given by the difference between the conversions calculated through the VOC disappearance and CO<sub>2</sub> appearance at temperatures below the ignition point, when reaction starts according to the (u) procedure (see Figs. 5 and 6). Our results with the Mn<sub>2</sub>O<sub>3</sub>/Al<sub>2</sub>O<sub>3</sub> (C) catalyst suggest that retained acetone could deactivate specific sites on the surface. In fact, as it can be seen in Fig. 6, a considerable CO<sub>2</sub> production is readily detected in the stream coming from the reactor at 423 K when oxidation is performed over the fresh surface of this catalyst (start-up procedure (u)). However, a comparable amount of CO<sub>2</sub> is produced only when the reaction temperature attains 453 K if the same catalyst was previously in contact with the acetone-air mixture (start-up procedure (s)).

#### 3.3.4. Exothermicity

Another important point that must be considered to understand the behaviour of the systems studied in this work is the exothermic character of the oxidation reaction. The ignition process will produce an important local temperature rise in the catalytic bed over that of the programmed ramp of the furnace. This has been

measured placing the thermocouple not at the entry but on the top of the catalyst bed. It has been seen that a temperature runaway of around 100 K occurs for toluene oxidation at the same time as the CO<sub>2</sub> and H<sub>2</sub>O peaks appear.

Therefore, a sort of chain reaction involving the combustion, the VOC adsorption–desorption on the support, its reaction and CO<sub>2</sub> desorption can be produced simultaneously. During the first stages of the ignition curve, at low temperatures, the catalyst is able to adsorb the VOC, thus giving apparent conversions higher than 0, desorbing it at higher temperatures. However, if the catalyst is active enough, the start of the oxidation of the organic molecule at low temperatures will coincide with the VOC molecules being adsorbed on the catalyst. Furthermore, if the oxidation reaction occurs at low temperature, part of the products themselves will be adsorbed on the catalyst as soon as they are formed. The oxidation reaction is an exothermic process, and it will produce a local rise in the catalyst temperature leading to the desorption of the reactant (VOC) and the products (H<sub>2</sub>O and CO<sub>2</sub>). The desorbed VOC can be oxidised producing more heat of reaction, and desorbing more adsorbed molecules at the same time. The CO<sub>2</sub> peaks will be the result of the coupling of all those processes at close temperatures.

Cordi et al. [23] had already accounted for the adsorption of the VOC on Al<sub>2</sub>O<sub>3</sub> before its oxidation over Pd, but they had not seen the coupling of the adsorption–desorption and oxidation processes. Similarly, Bowker et al. [24] had searched on the explosive characteristics of acetate groups adsorbed on Rh/Al<sub>2</sub>O<sub>3</sub> leading to a CO<sub>2</sub> peak. Probably the autocatalytic process involved in their work is the same taking place in our experiments. Some authors have dealt with the negative effect of H<sub>2</sub>O and CO<sub>2</sub> on the catalytic activity of Pd/Al<sub>2</sub>O<sub>3</sub> [25]. A possible explanation could be found in the occupancy of the VOC adsorption sites of the Al<sub>2</sub>O<sub>3</sub> by CO<sub>2</sub>, as we have seen that both are adsorbed at close temperatures. As a result CO<sub>2</sub> would appear as a poison, losing its poisoning activity at higher temperatures, when CO<sub>2</sub> is no more adsorbed.

In order to check our hypothesis, the fractional conversion of the reaction calculated by following the concentration of toluene and both combustion products was plotted and integrated as a function of time

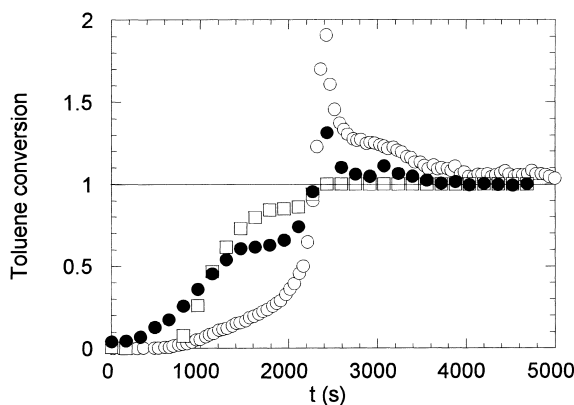


Fig. 7. Toluene fractional conversion over reduced Pd/Al<sub>2</sub>O<sub>3</sub> followed by the toluene disappearance (□) and the water (●) and CO<sub>2</sub> (○) appearance over time.

in Fig. 7. The difference in the integration values obtained for the toluene and the CO<sub>2</sub> signals before 2300 s, before the occurrence of the peak, results in  $3.3 \times 10^{19}$  molecules of toluene. On the other hand, the integration of the CO<sub>2</sub> peak indicates that the excess of CO<sub>2</sub> comes from  $3.1 \times 10^{19}$  molecules of toluene. Taking into account the lack of accuracy inherent to the method used (in particular, the time constant of the CO<sub>2</sub> detector available makes it difficult to evaluate the height of the sharp CO<sub>2</sub> peak), the good agreement confirms the hypothesis of the adsorption of toluene and its products below 450 K, and the desorption above 450 K. Considering the Pd dispersion (32%) and the amount of catalyst loaded (200 mg), there are  $3.6 \times 10^{18}$  surface atoms of Pd. On the other hand, there are  $5 \times 10^{19}$  nm<sup>2</sup> of Al<sub>2</sub>O<sub>3</sub>. Therefore, it can be said that toluene, or the species derived from the adsorption of toluene are located mainly on the support, and not on the palladium particles.

The importance of the combustion temperature can be illustrated by Fig. 8 where the toluene ignition curves for differently prepared and calcined Pd/Al<sub>2</sub>O<sub>3</sub> catalysts have been included. As it can be seen the activity of the A catalyst is the highest one, and its CO<sub>2</sub> peak is the biggest one as well. When passing from sample A to D the activity decreases, leading to higher *T*<sub>50</sub> values and less intense CO<sub>2</sub> peaks. Therefore, as activity increases and oxidation temperatures approach those at which the adsorption–desorption phenomena occur, the conversion surpasses from 100% is more im-



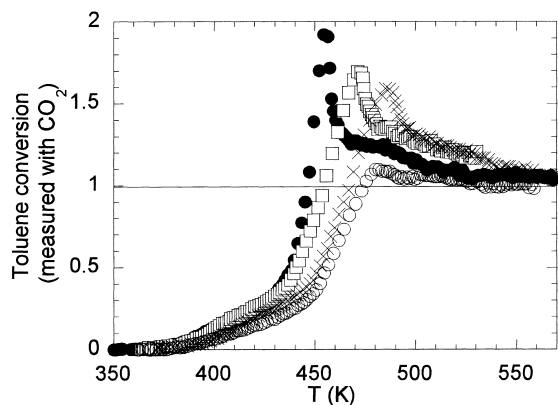


Fig. 8. Ignition curves of toluene over different reduced Pd/Al<sub>2</sub>O<sub>3</sub> catalysts: A (●), B (□), C (×), D (○). The fractional conversion was calculated following the CO<sub>2</sub> appearance.

portant. The same behaviour can be appreciated for acetone combustion over supported Mn<sub>2</sub>O<sub>3</sub> catalysts. In fact, Mn<sub>2</sub>O<sub>3</sub>/Al<sub>2</sub>O<sub>3</sub> (C) is the most active among the prepared manganese-based catalysts and exhibits also the most intense CO<sub>2</sub> peak. Interestingly a correlation seems to exist between the amount of acetone retained and the intensity of the corresponding CO<sub>2</sub> peak. This suggests that for this system the simultaneous desorption and combustion of the retained acetone could play a major role in the observed phenomena.

Finally and as a conclusion of the analysis of the phenomena presented in this article, some suggestions can be proposed to overcome this kind of problems. The first one is to work under steady-state conditions, obtaining the ignition curves increasing the temperature stepwise and waiting for the equilibrium to be achieved at each temperature. The second one is to work in a reverse way, starting the reaction at high temperature and cooling down with a programmed ramp. Nevertheless, it must be pointed out that the later proposal, even if much quicker than the former, is only useful for samples stable under reaction conditions in all the temperature range, and this is not the case for Pd/Al<sub>2</sub>O<sub>3</sub> after H<sub>2</sub> pretreatment at 573 K. As a conclusion of the study of the effect of the start-up procedure, it could be more convenient to obtain the ignition curves after a previous contact period of the VOC-air mixture with the catalysts (start-up procedure (s)) and to calculate the conversion from VOC disappearance data.

#### 4. Conclusions

In this work complete oxidation of toluene over Pd/Al<sub>2</sub>O<sub>3</sub> and that of acetone over supported Mn<sub>2</sub>O<sub>3</sub> catalysts have been studied. In both cases, some of the ignition curves have presented CO<sub>2</sub> peaks showing conversions higher than 100% when measured through CO<sub>2</sub> appearance in the products stream. In addition, disagreements between the conversion values calculated by means of the VOC and CO<sub>2</sub> analyses have been found as well.

After discarding the formation of partial oxidation products and the hydrogen retention on Pd as possible causes, the adsorption–desorption of VOCs, surface reaction intermediates and CO<sub>2</sub> were considered. It can be said that when the activity of the active phase is high enough to start the oxidation at a sufficiently low temperature, close to that at which the adsorption and desorption of the different species take place, all these processes will be coupled giving rise to the above-cited phenomena. The coupling of these phenomena is strongly enhanced by the exothermic character of VOCs combustion. As a result, ignition curves must be considered in a deeper way before taking out general conclusions about the catalytic activity of the considered catalyst for complete oxidation of VOCs.

#### Acknowledgements

Financial support by CICYT (QUI97-1040-CO3), Gobierno Vasco (M. Paulis Ph.D. scholarship), UPV/EHU, Diputación Foral de Gipuzkoa, CONICET (J. Sambeth postdoctoral fellowship), Universidad Pública de Navarra and Gobierno de Navarra (O.F. 557-1996 and 143/1998) are gratefully acknowledged. L.M. Gandía and A. Gil acknowledge Dr. M.A. Vicente for XRD and BET surface area measurements.

#### References

- [1] J.J. Spivey, in: J.R. Anderson, M. Boudart (Eds.), Complete Oxidation of Volatile Organics, Catalysis, Vol. 8, The Royal Society of Chemistry, Cambridge, 1989, p. 158.
- [2] S.K. Agarwal, J.J. Spivey, *Env. Progress* 12 (1993) 182.
- [3] C.F. Cullis, B.M. Willatt, *J. Catal.* 83 (1983) 267.
- [4] P. Papaefthimiou, T. Ioannides, X.E. Verykios, *Appl. Catal. B: Environ.* 13 (1997) 175.

- [5] R. Prasad, L.A. Kennedy, E. Ruckenstein, *Catal. Rev.-Sci. Eng.* 26 (1984) 1.
- [6] M.F.M. Zwinkels, S.G. Järås, P.G. Menon, T.A. Griffin, *Catal. Rev.-Sci. Eng.* 35 (1993) 319.
- [7] J.L.G. Fierro, *Catal. Today* 8 (1990) 153.
- [8] N. Yamazoe, Y. Teraoka, *Catal. Today* 8 (1990) 175.
- [9] T. Seiyama, *Catal. Rev.-Sci. Eng.* 34 (1992) 281.
- [10] C.J. Heyes, J.G. Irwin, H.A. Johnson, R.L. Moss, *J. Chem. Tech. Biotechnol.* 32 (1982) 1025.
- [11] S. Imamura, K. Fukuda, T. Nishida, T. Inui, *J. Catal.* 93 (1985) 186.
- [12] C. Lahousse, A. Bernier, P. Grange, B. Delmon, P. Papaefthimiou, T. Ioannides, X. Verykios, *J. Catal.* 178 (1998) 214.
- [13] J. Benítez, J. Carrizosa, J.A. Odriozola, *J. Appl. Spectrosc.* 46 (1993) 1360.
- [14] K.I. Muto, N. Katada, M. Niwa, *Appl. Catal. A: General* 134 (1996) 203.
- [15] A.A. Davydov, in: C.H. Rochester (Ed.), *Infrared Spectroscopy of Adsorbed Species on the Surface of Transition Metal Oxides*, Wiley, Chichester, 1990.
- [16] G. Busca, E. Finocchio, V. Lorenzelli, G. Ramis, M. Baldi, *Catal. Today* 49 (1999) 453.
- [17] A.B. Azimov, V.P. Vislovskii, E.A. Mamedov, R.G. Rizayev, *J. Catal.* 127 (1991) 354.
- [18] G. Busca, *Catal. Today* 27 (1996) 457.
- [19] G. Busca, E. Finocchio, G. Ramis, G. Ricchiardi, *Catal. Today* 32 (1996) 133.
- [20] S. Lars, T. Andersson, *J. Catal.* 98 (1986) 138.
- [21] E. Finocchio, G. Busca, V. Lorenzelli, V. Sanchez Escibano, *J. Chem. Soc. Faraday Trans.* 92 (1996) 1587.
- [22] A.G. Panov, J.J. Fripiat, *J. Catal.* 178 (1998) 188.
- [23] E.M. Cordi, J.L. Falconer, *J. Catal.* 162 (1996) 104.
- [24] M. Bowker, T.J. Cassidy, *J. Catal.* 174 (1998) 65.
- [25] R. Burch, F.J. Urbano, P.K. Loader, *Appl. Catal. A: General* 123 (1995) 173.